Electrical, elastic properties and defect structures of isotactic polypropylene composites doped with nanographite and graphene nanoparticles

L.V. Elnikova[1], A.N. Ozerin[2], V.G. Shevchenko[2], A.T. Ponomarenko[2], P.M. Nedorezova[3], O.M. Palaznik[3], V.V. Skoi[4,5], A.I. Kuklin[4,5]

[1] Alikhanov Institute for Theoretical and Experimental Physics, Kurchatov institute, Moscow,
[2]Enikolopov Institute of Synthetic Polymeric Materials, RAS, Moscow,
[3]Semenov Federal Research Center for Chemical Physics, RAS, Moscow,
[4]Joint Institute for Nuclear Research, Dubna
[5]Moscow Institute of Physics and Technology, Dolgoprudny,
Russian Federation

ICIFMS-19 Moscow-Rome 2022

Outline:

- Introduction
- Manufacturing and characterization of samples with DMA, dielectric spectroscopy and SANS
- Cosserat theory and fractons
- Modeling and results
- Conclusions

Abstract: We study elastic properties of graphene- and nanographite doped polymer iPP composites connecting with their electric properties and morphology. To explain these correlations, we study defect structures in the bulk of iPP matrix in terms of the theory of Cosserat elasticity and fractons.

Motivation:

Polymers filled with carbon allotropes (graphene (GNP), nanographite) have wide engineering applications in optoelectronics, photonics, sensing materials and actuators *etc*., because adding of nanofillers improves their functional properties (e.g. increasing the conductivity of the resulting composites by several orders of magnitude).

Polymer nanocomposites like iPP-GNP and iPP-nanographite systems demonstrate percolation thresholds at low volume fraction of nanofillers.

Precise prediction of their physical properties serves for the further design of nanocomposites.

Manufacturing of nanocomposites

and their geometrical parameters

The samples of iPP with 60% crystallinity are filled by *in situ* polymerization with GNP at concentrations of 0.7 and 1.8 wt%, nanographite at 1.5 and 3.6 wt%. Metallocene catalyst is used.

V.G. Shevchenko, S.V. Polschikov, P.M. Nedorezova, A.N. Klyamkina, A.N. Shchegolikhin, A.M. Aladyshev, V.E. Muradyan, Polymer 53 (2012) 5330, J Applied Polymer Sci. 127 (2013) 904, Polym. Sci. Ser. A 46 (2004) 242, Nanotech. in Russia 9(3-4) (2014) 175, *ibid* 8(1-2) (2013) 69

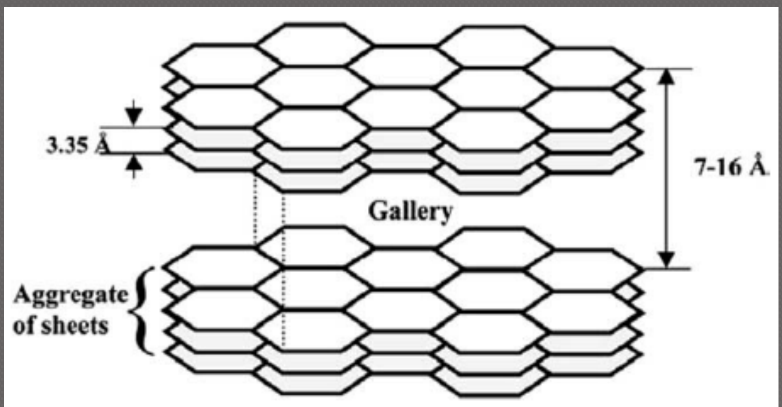

Schematic view of the graphite layer structure

Initial sizes:
GNP (100×100×1.127) nm
Nanographite (100×100×47.3) nm

Resulting sizes:
GNP wafers with a thickness of 1–20 nm (3-5 layers)

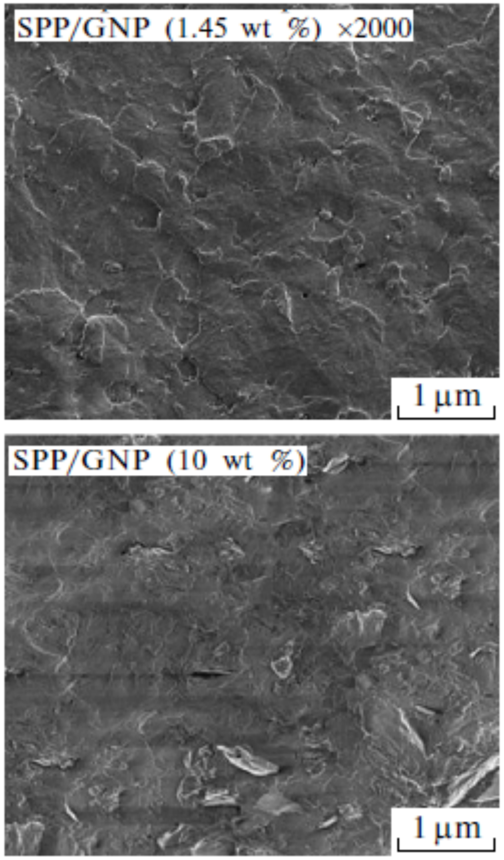

SEM micrographs of chips of nanocomposite films in liquid nitrogen

1. Dynamic mechanical analysis (DMA)

M.A. Milani *et al* Composites Science and Technology 84 (2013) 1–7

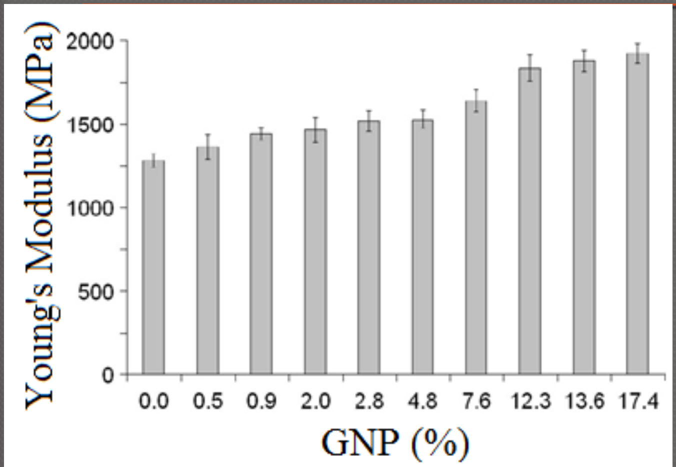

β relaxation is associated with generalized motion in the amorphous regions during the glass transition,

γ relaxation address to the mobility of crystallites

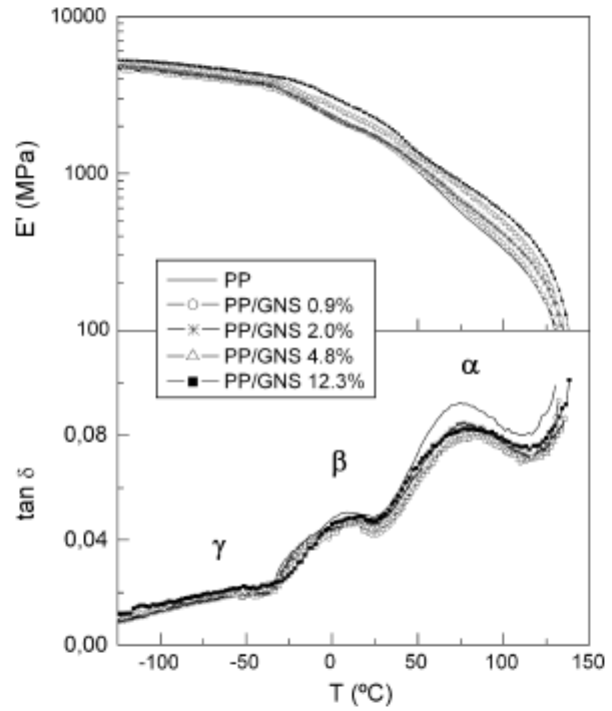

S.V. Polshchikov, P.M. Nedorezova, O.M. Komkova, A.N. Klyamkina, A.N. Shchegolikhin, V.G. Krasheninnikov, A.M. Aladyshev, V.G. Shevchenko, V.E. Muradyan, Nanotechnologies in Russia, 9(3–4)(2014)175 :

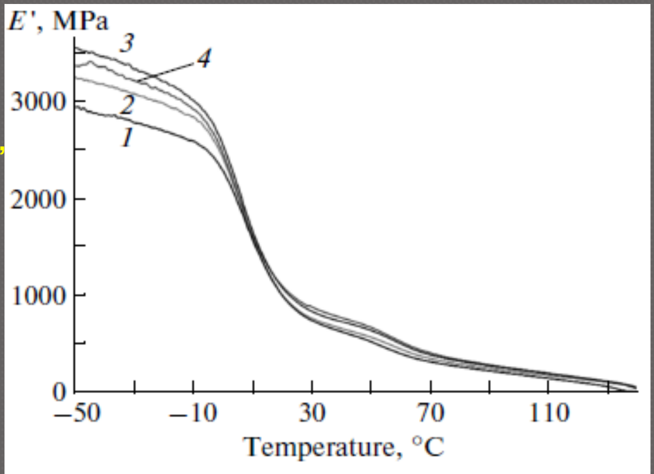

Temperature dependences of the dynamic modulus of SPP and its composites with GNP: (*1*) SPP, (*2*) 0.4, (*3*) 1.45, and (*4*) 3.7 wt % GNP.

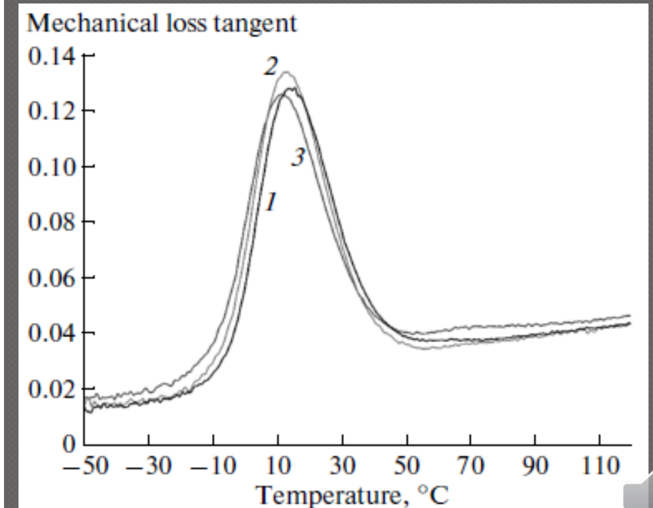

The temperature dependence of the mechanical loss tangent for composites (a) SPP/GNP: (*1*) SPP, (*2*) 0.4 wt % GNP, and (*3*) 3.7 wt % GNP

Results of experiments

2. Dielectric spectroscopy

S.V. Polschikov, P.M. Nedorezova, A.N. Klyamkina, A.A. Kovalchuk, A.M. Aladyshev, A.N. Shchegolikhin, V.G. Shevchenko, V.E. Muradyan. J. Appl. Polym. Sci. 2012, DOI: 10.1002/APP.37837

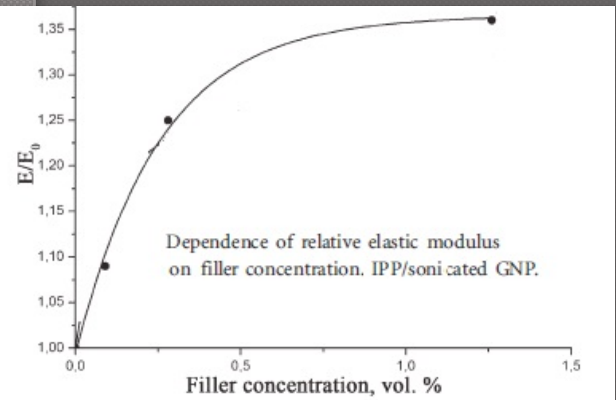

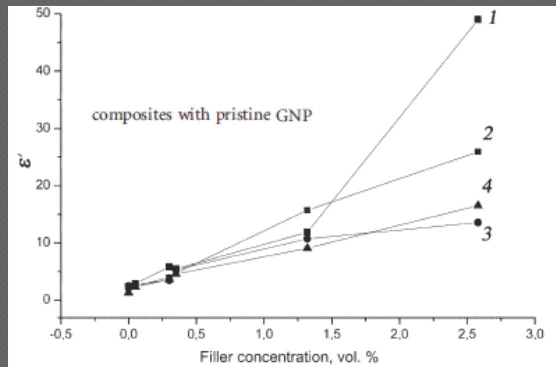

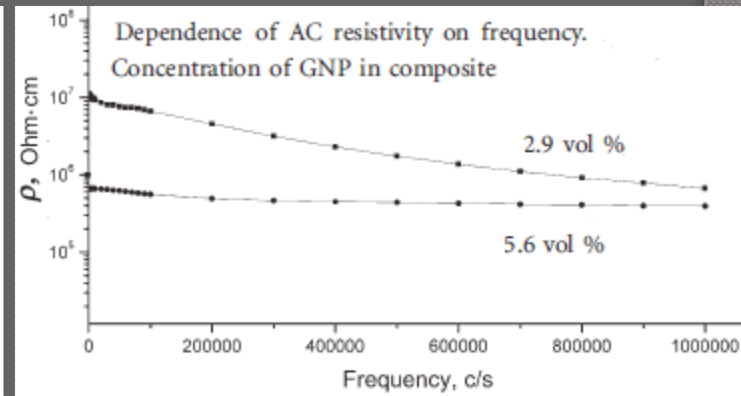

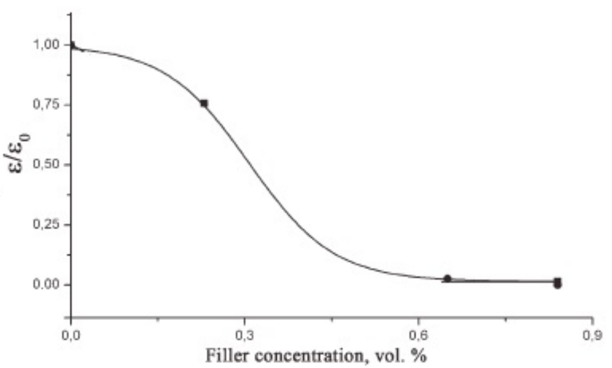

Dependence of relative elongation at break on filler concentration. IPP/sonicated GNP.

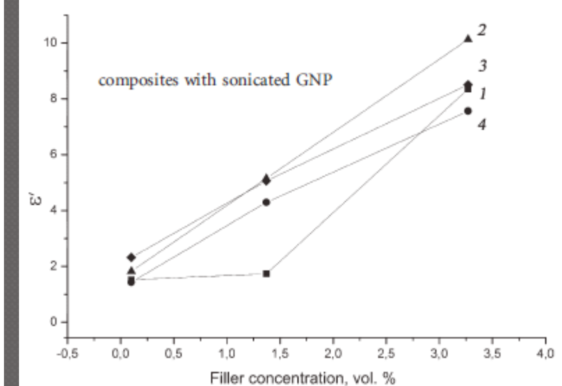

Concentration dependence of dielectric permittivity at different frequencies (1–3.2 GHz, 2–4.8 GHz, 3–6.6 GHz, 4–11 GHz)

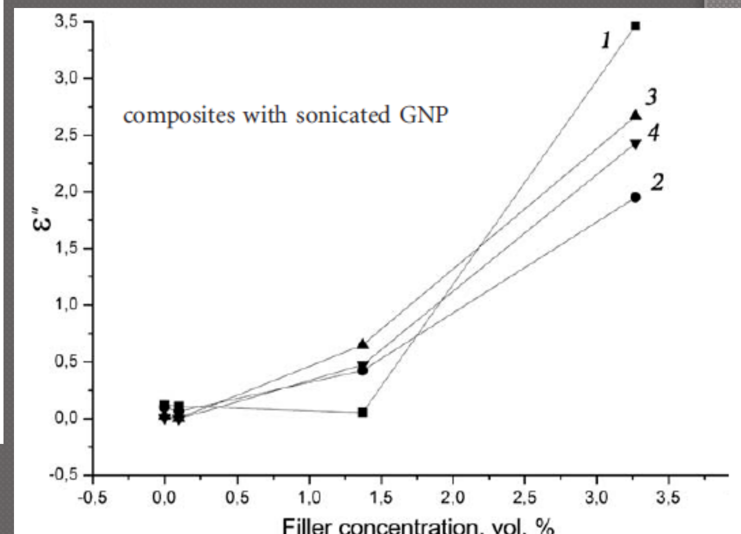

Concentration dependence of dielectric losses at different frequencies (1–3.2 GHz, 2–4.8 GHz, 3–6.6 GHz, 4–11 GHz)

Polymer composites with graphene exhibit low values of percolation threshold, i.e., concentration of filler where sharp increase of electrical conductivity occurs

3. Small-angle neutron scattering (SANS)

Fullerenes, nanotubes and carbon nanostructures, 2021, https://doi.org/10.1080/1536383X.2021.1896496

SANS is nondestructive and applicable for a identifiable phenomenon at aggregation scale >1 Å

To define morphology of GNP's and nanographite particles and their aggregates in the bulk of iPP, we used direct method SANS at the YuMO spectrometer at IBR2, Dubna, Russia, with characteristics:

Neutron wavelength λ= 0.7–6Å

Flux on a sample ~10^7 n/(s×cm^2)

With SANS we can identify fractal structures of nanoparticles and aggregates and choose a universality class and a further theoretical model with defects

S. Alexander, C. Laermans, R. Gorbach, and H.M. Rosenberg, Phys. Rev. B. 28(1983)4615

SANS

Fullerenes, nanotubes and carbon nanostructures, 2021, https://doi.org/10.1080/1536383X.2021.1896496

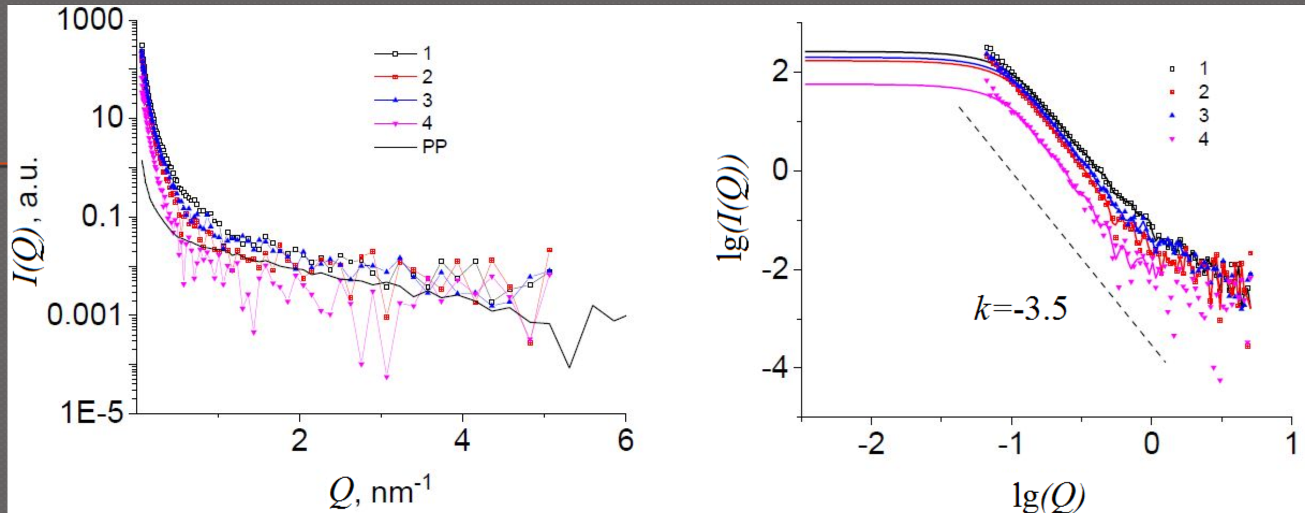

$d_s = 6 - |k| = 2.5$
fractal
dimensionality

The experimental SANS intensity $I(Q)$ of the nanographite (1,2-3.6 and 1.5 wt%),GNP (3,4 -1.8 and 0.7 wt%) samples

To determine the shape and
spatial structure of scattering
particles we used
procedures of ATSAS 2.4 software

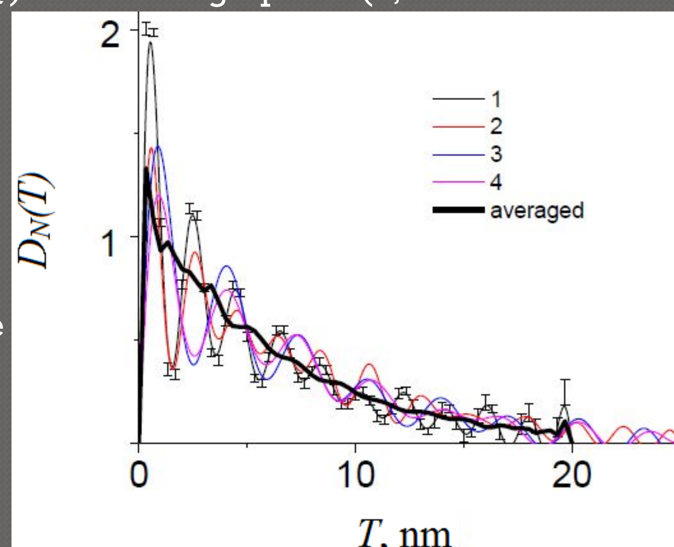

Initial plates:
GNP (100×100×1.127) nm
Nanographite (100×100×47.3) nm

Resulting sizes:
GNP wafers with a thickness
of 1–20 nm (3-5 layers)

Normalized distribution functions of particle thicknesses D_N under the assumption of a polydisperse system of plate-shaped particles with a thickness T calculated from the scattering curves for GNP and nanographite particles.

Defects of a graphene (graphite) lattice

A.I. Podlivaev and L.A. Openov, JETP Letters, 106(2) (2017) 110, O.V. Yazyev and S.G. Louie, Phys Rev B 81(210) 195420,P.Surowka, M.Katsnelson, Vl.Osipov, M.Volzmediano (arXiv:cond-mat/0612343v1)

Pentagons and heptagons in a graphite sheet are a topological defects…
Actually, fivefold coordinated particles (pentagons) are orientational disclination defects in the otherwise sixfold coordinated triangular lattice.

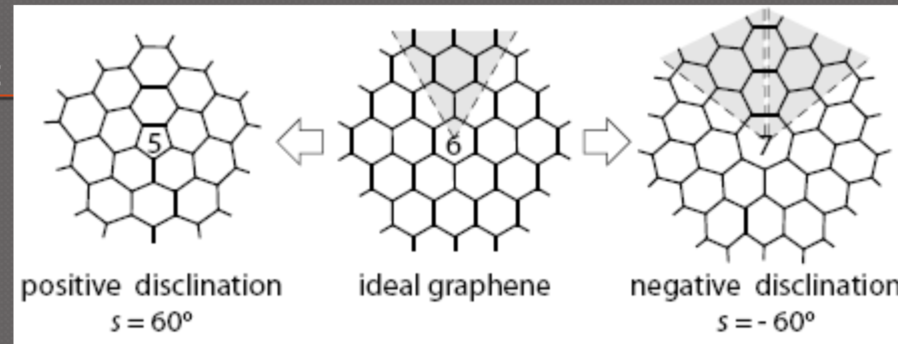

Positive and negative disclinations in graphene are produced by either removing or adding a 60° wedge (shaded area) of material without changing the coordination of carbon atoms.

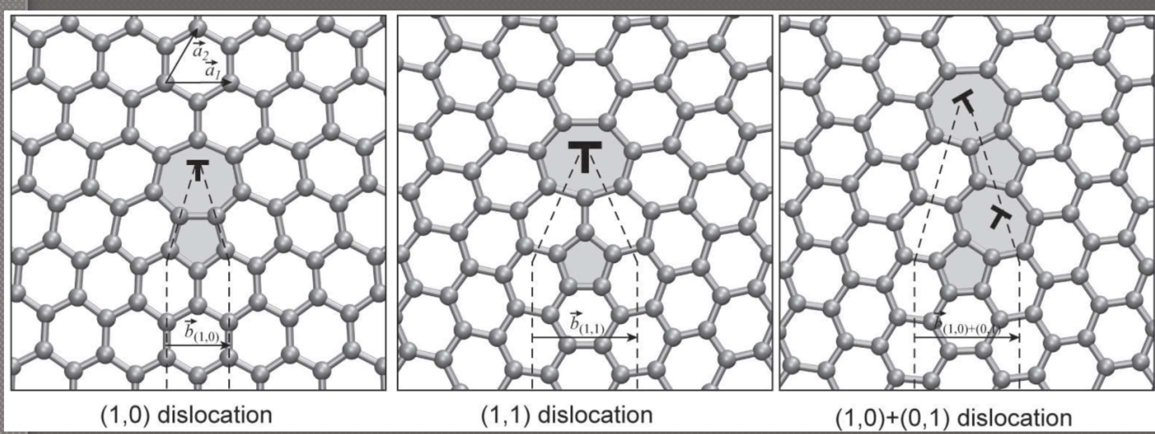

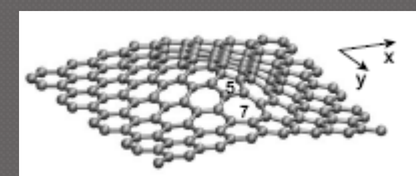

Dipole pairs 5-7 form linear defects

Energetics of topological defects (O.V. Yazyev and S.G. Louie): the Read-Shockley equation for grain boundaries

$$\gamma(\theta') = \frac{\mu|\vec{b}|}{4\pi(1-\nu)}\theta'\left(1 + \ln\frac{|\vec{b}|}{2\pi r_0} - \ln\,\theta'\right),$$

where μ is the shear modulus, ν the Poisson's ratio, r_0 is the core radius encompasses the energy of the dislocation core (=0.95-1.2Å)

Cosserat elasticity

This is a generalized theory of elasticity, known as micropolar or Cosserat elasticity.
In Cosserat theory, a local element of an elastic body is described in terms of local displacement and local orientation. Cosserat theory has a microscopic origin

Upon the duality transformation these two degrees of freedom map onto a coupled theory of a U(1) vector-valued one-form gauge field and an ordinary U(1) gauge field. In terms of gauge theory, it is possible to discuss the defect matter.

Applications for graphene: gauge theory with curvature effects and with the membrane theory E.A. Kochetov and V.A. Osipov, J. Phys. A 32, 1961 (1999); by them and P. Pincak, Electronic properties of disclinated flexible membrane beyond the in extensional limit: application to graphene, J. Phys.: Condens. Matt. 22 (2010) 395502-1; M.A.H. Vozmediano, M.P. Lopez-Sancho, T. Stauber, and F. Guinea, Phys. Rev. B 72, 155121 (2005); M.A.H. Vozmediano, M.I. Katsnelson, F. Guinea, Phys. Rep., 496(2010)109; O.V. Yazyev, S.G. Louie, Topological defects in graphene: Dislocations and grain boundaries, Phys. Rev. B. 81 (2010) 195420-1; I.A. Fialkovsky, M.A. Zubkov Symmetry 12(2020)317

Applications for crystalline polymers
G. Corazza1, and R. Singh, arXiv:2109.09173v3 [cond-mat.stat-mech] 23 Sep 2021

In Cosserat theory, the stress tensor is not symmetric.
Cosserat theory is not dual to a symmetric tensor theory. I.e.

Cosserat theory

P.Surowka. SciPost Phys. 8, 065 (2020)

The action is a functional of θ and u^i

$$S[u^i,\theta] = \int dt d^2x \left[\dot{\theta}\dot{\theta} + \dot{u}^i\dot{u}^i - C^{ijkl}\gamma_{ij}\gamma_{kl} + \zeta\tau_i\tau^i\right]$$

C^{ijkl} and ζ correspond to elastic coefficients in the theory

$$Z = \int DuD\theta DPDTDLe^{iS[u,\theta,P,T,L]}$$

$$S = \int dt d^2x \left[P_iP^i + (L_0)^2 + \zeta^{-1}L_iL^i + C^{-1}_{ijkl}T^{ij}T^{kl} + u_i\left(\partial_\mu T^{i\mu}\right) + \theta\left(\partial_\mu L^\mu - \epsilon^{ij}T_{ij}\right)\right]$$

Integrating out (the smooth part of) θ and u_i leads to the following constraints

$$\partial_\mu T^{i\mu} = 0\,, \qquad \partial_\mu L^\mu - \epsilon^{ij}T_{ij} = 0\,.$$

resolve the constraints by introducing the gauge fields

The stress tensor is $T^{ij} = C^{ijkl}u_{kl}$

C^{ijkl} is a tensor of elastic moduli

Lets introduce dual gauge theory:

$P^i = \epsilon^{kl}\partial_k A^i_l\,, \qquad T^{ij} = \epsilon^{jk}(-\partial_0 A^i_k + \partial_k \Phi^i)$ a notation $\Phi^i = A^i_0$

$B^i = \epsilon^{kl}\partial_k A^i_l\,, \qquad E^i_j = \epsilon^i{}_k(-\partial_0 A^k_j + \partial_j \Phi^k)$ the generalized electric and magnetic fields

A resulting source-free action is

$$S = \int dt d^2x \left[\tilde{C}^{-1}_{ijkl}E_{ij}E_{kl} + B_iB^i + \zeta^{-1}(\epsilon^{ij}A_{ij})^2 - \Phi^i\Phi_i\right]$$

This action has two gapless and one gapped mode. The gapped mode is the anti-symmetric part of A_{ij} with the mass being fixed by the stiffness of the local orientation, ζ, whereas the remaining components are gapless.

Defects in dual formulation

$$\rho_{\rm vac} = \partial_i u^i\,, \quad \rho^i_{\rm disl} = \epsilon^{kl}\partial_k\partial_l u^i_{\rm sing}\,, \quad \rho_{\rm disc} = \epsilon^{ij}\partial_i\partial_j\varphi$$

$$\rho_\theta = \epsilon^{ij}\partial_i\partial_j\theta$$

P.Surowka. SciPost Phys. 8, 065 (2020)

$$\rho_{rot} = \rho_{discl} + \rho_\theta = \varepsilon^{ij}\partial_i\partial_j(\varphi+\theta)$$

The total defect density

These disclination defects have two independent contributions

$$\gamma_{ij} = \frac{1}{2}(\partial_i u_j + \partial_j u_i) + \frac{1}{2}(\partial_i u_j - \partial_j u_i) + \epsilon_{ij}\theta = u_{ij} + \epsilon_{ij}(\varphi+\theta)$$

the asymmetric strain tensor in terms of the angles

The coupling of $u^i_{\rm sing}$ and $\theta_{\rm sing}$ to the gauge fields

$$\delta S = \int dtd^2x\Big[(\rho^i + 2\epsilon^{ij}\partial_j\theta_{\rm sing})\Phi_i + (J^{ij} + 2\dot\theta_{\rm sing}\epsilon^{ij})A_{ij} + j^\mu a_\mu\Big]$$

where $j^0 = \rho_\theta = \epsilon^{ik}\partial_k\partial_i\theta_{\rm sing}\,, \qquad j^i = \epsilon^{ij}\left(\partial_i\partial_0 - \partial_0\partial_i\right)\theta_{\rm sing}$

The Gauss law in terms of canonical momenta is $\partial_i\pi^i = \rho_\theta, \quad \partial_j\Pi^{ij} = \rho^i - e^i\,,$

where the density of θ-vortices $\varrho = j^0 = \epsilon^{ij}\partial_i\partial_j\theta$.

$\partial_i\partial_j\Pi^{ij} = \partial_i\rho^i + \rho_\theta = \rho_{\rm rot}$ the Gauss law constraint equations

both angle singularities and displacement singularities con tribute to disclinations (or to the “scalar charge”)

The dipole moment $D_i = \int x_i(\partial_j\rho^j + \rho_\theta) = \int \rho^i + \int x^i\rho_\theta = \int \partial(\ldots) = 0$

but $\int \rho^i = -\int x^i\rho_\theta$ and are not separately conserved

Cosserat elasticity and fractons

- M. Pretko, L. Radzihovsky. Phys. Rev. Lett. 120(19)(2018)195301. Fracton-Elasticity Duality; PRB 100(2019)134113,
- A.Gromov, P. Surowka, On duality between Cosserat elasticity and fractons.SciPost Phys. 8 (2020) 065,
- K. T. Grosvenor1, C.Hoyos, F. Peña-Benítez and P. Surówka, Front. Phys.9(2022)792621

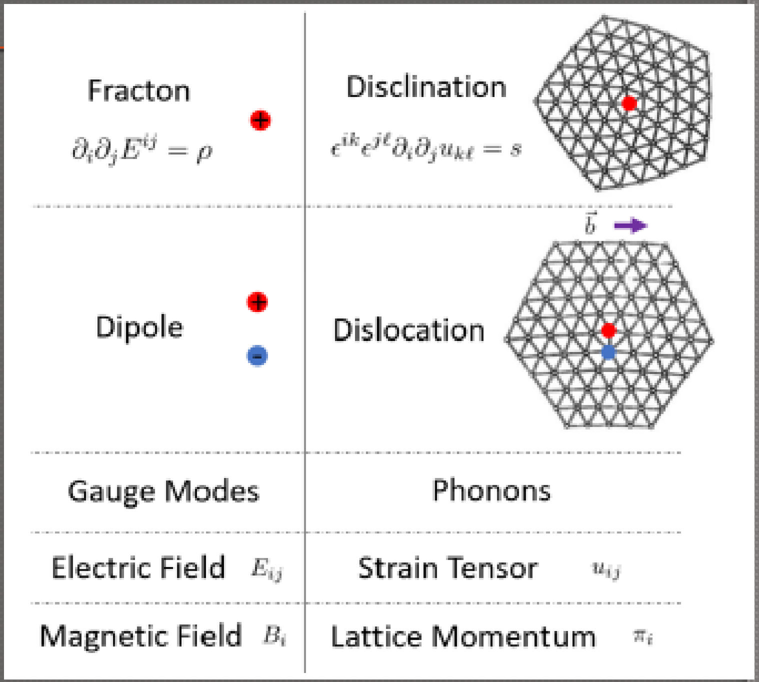

Pretko and Radzihovsky discovered that a tensor gauge theory in two dimensions can be mapped to a familiar theory of elasticity where the fractonic excitations correspond to topological defects. Their theory is based on the earlier works of Kleinert that pioneered the field of elastic dualities in the 1980s

Our SANS data serve to ground an application of a fracton model (S. Alexander, C. Laermans, R. Gorbach, and H.M. Rosenberg, Phys. Rev. B. 28(1983)4615)

Fracton formulation

K. T. Grosvenor1, C.Hoyos, F. Peña-Benítez and P. Surówka, Front. Phys.9(2022)792621

The action for the dual gauge fields

$$S=\int dtd^2x\left[\tilde{C}^{ijkl}E_{ij}E_{kl}+B_iB^i+\zeta^{-1}\left(b+\epsilon^{ij}A_{ij}\right)^2+\left(e^i-A_0^i\right)\left(e_i-A_{i0}\right)\right].$$

It is invariant under the following set of transformations

$$\delta a_\mu=\partial_\mu\lambda$$

$$\delta A_{i0}=\partial_0\alpha_i,\qquad \delta A_{ij}=\partial_j\alpha_i,\qquad \delta a_i=-\alpha_i,\qquad \delta a_0=0.$$

The charges of the dual theory correspond to defects in Cosserat elasticity

$$\mathcal{L}_{\text{sources}}=\rho^i_{\text{rot}}A_{i0}+J^{ij}_{\text{rot}}A_{ij}+a_0\rho_\theta+a_ij_i=\left[\left(\rho^i+2\epsilon^{ij}\partial_j\theta_{\text{sing}}\right)A_{i0}+\left(J^{ij}+2\dot{\theta}_{\text{sing}}\epsilon^{ij}\right)A_{ij}+a_0\rho_\theta+a_ij_i\right],$$

$$\text{where } \rho_\theta=\epsilon^{ik}\partial_k\partial_i\theta_{\text{sing}},\ j^i=\epsilon^{ik}\left(\partial_k\partial_0-\partial_0\partial_k\right)\theta_{\text{sing}}.$$

The dislocation density has contributions from singularities of both the displacement and orientation fields. As such, in order to correctly account for fractonic behavior of defects, in Cosserat theory both contributions have to be taken into account

Results of numerical modeling

(27) $H = \int d^2x \frac{1}{2}\left(C^{ijkl}u^{ij}u^{kl} + \pi^i \pi_j\right)$ $Z = \int Du\, exp(-H/k_BT)$

M.Hering, H.Yan, and J.Reuther Phys Rev.B. 104, 064406 (2021)

$$\frac{3}{16}\frac{\alpha}{d^2}\sum_{ij}\left(r_{ij}^2 - d_{cc}^2\right)^2 + \frac{3}{8}\beta d_{cc}^2\sum_{ijk}\left(\theta_{ijk} - \frac{2\pi}{3}\right)^2 + \gamma\sum_{ijkl} r_{i,jkl}^2$$

r_{ij} are the distances between two bond atoms,
α = 26.060 eV/Å, β = 5.511 eV/Å^2, and γ = 0.517 eV/Å^2

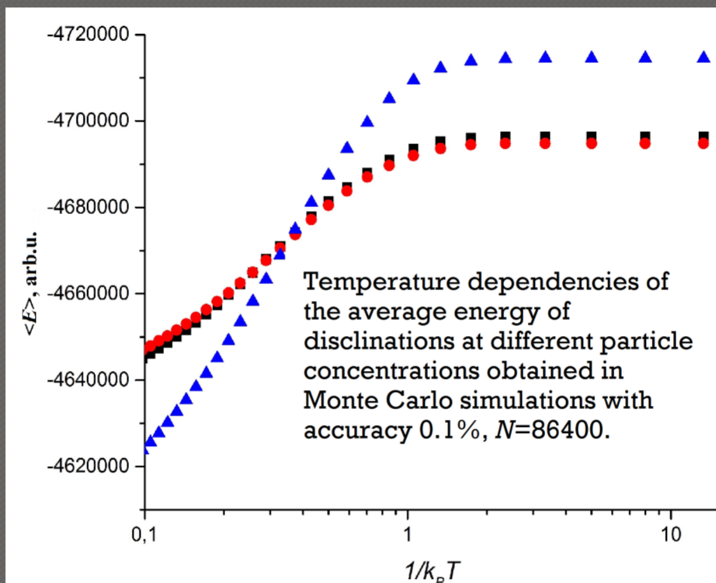

Temperature dependencies of the average energy of disclinations at different particle concentrations obtained in Monte Carlo simulations with accuracy 0.1%, N=86400.

The immobility stems from the fact that fractons can only be created at the corners of a membranelike operator, known as type-I scenario

Hering et al. proved these facts with classical numerical Monte-Carlo simulations for the 3-states Potts model on kagome lattice.

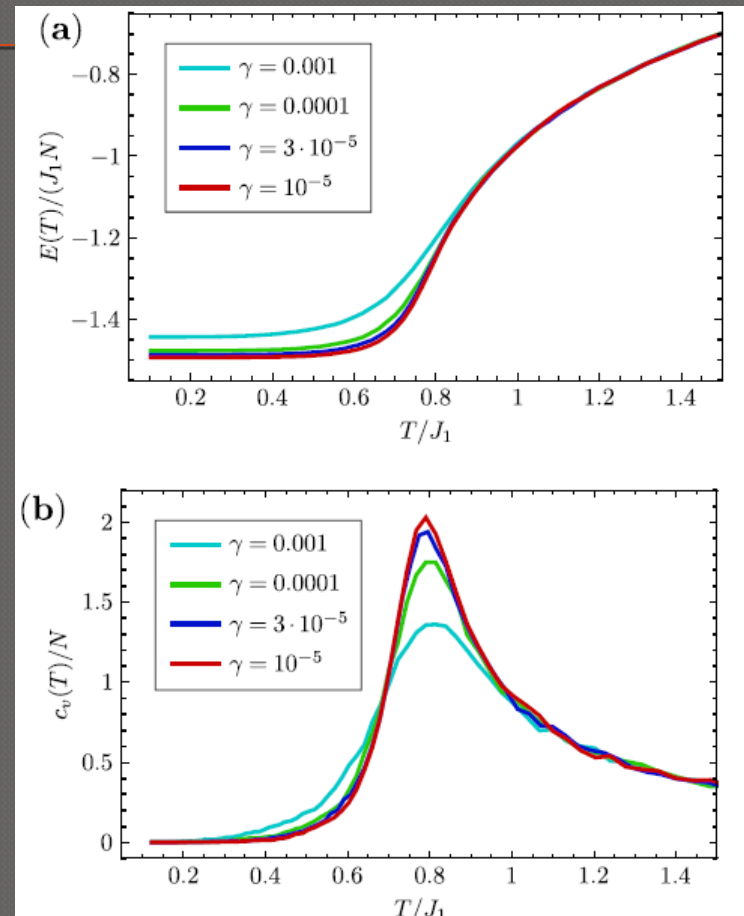

(a) Energy per site $E(T)/(J_1N)$ for the three-state Potts model at constant system size $L = 100$ and varying cooling rates γ. (b)

(b) Specific heat per site $c_v(T)/N$ of the three-state Potts model for different γ and constant $L = 100$.

Conclusions

1. To explain observed aggregation of GNP and nanographite sheets in iPP, we proposed the Cosserat type model and associate aggregation with interactions of disclinations in graphene (graphite) and interactions of sheet edges in the iPP matrix via the tunnel effect.

2. The type 1 fracton model is an appropriate to realize the Cosserat elasticity principles in the case of the polymer composites like iPP/GNP and iPP/nanographite composites

3. All the modeling parameters of the dual theory may be expressed in observables in DMA, DE, SANS

Details of this talk are in https://arxiv.org/abs/2205.15392

Thank you for your attention !